2013

An all-electron density functional theory study of the structure and properties of the neutral and singly charged M-12 and M-13 clusters: M = Sc-Zn

G. L. Gutsev
Florida A&M University, gennady.gutsev@famu.edu

C. W. Weatherford
Florida A&M University

K. G. Belay
Florida A&M University

B. R. Ramachandran
Louisiana Tech University

P. Jena
Virginia Commonwealth University, pjena@vcu.edu

An all-electron density functional theory study of the structure and properties of the neutral and singly charged M_{12} and M_{13} clusters: M = Sc–Zn

G. L. Gutsev,[1,a)] C. W. Weatherford,[1] K. G. Belay,[1] B. R. Ramachandran,[2] and P. Jena[3]
[1]*Department of Physics, Florida A&M University, Tallahassee, Florida 32307, USA*
[2]*College of Engineering and Science, Louisiana Tech University, Ruston, Louisiana 71272, USA*
[3]*Department of Physics, Virginia Commonwealth University, Richmond, Virginia 23284, USA*

(Received 6 February 2013; accepted 21 March 2013; published online 22 April 2013)

The electronic and geometrical structures of the M_{12} and M_{13} clusters where M = Sc, Ti, V, Cr, Mn, Fe, Co, Ni, Cu, and Zn along with their singly negatively and positively charged ions are studied using all-electron density functional theory within the generalized gradient approximation. The geometries corresponding to the lowest total energy states of singly and negatively charged ions of V_{13}, Mn_{12}, Co_{12}, Ni_{13}, Cu_{13}, Zn_{12}, and Zn_{13} are found to be different from the geometries of the corresponding neutral parents. The computed ionization energies of the neutrals, vertical electron detachment energies from the anions, and energies required to remove a single atom from the M_{13} and $M_{13}{}^{+}$ clusters are in good agreement with experiment. The change in a total spin magnetic moment of the cation or anion with respect to a total spin magnetic moment of the corresponding neutral is consistent with the one-electron model in most cases, i.e., they differ by $\pm 1.0\ \mu_B$. Exceptions are found only for $Sc_{12}{}^{-}$, $Ti_{12}{}^{+}$, $Mn_{12}{}^{-}$, $Mn_{12}{}^{+}$, $Fe_{12}{}^{-}$, $Fe_{13}{}^{+}$, and $Co_{12}{}^{+}$. © *2013 American Institute of Physics*. [http://dx.doi.org/10.1063/1.4799917]

I. INTRODUCTION

Transition metal clusters M_n possess many exceptional properties[1] and have been the subject of numerous studies by experimental and theoretical groups. Due to their unfilled *d*-shells, transition metal clusters carry magnetic moments and can couple magnetically even though they are nonmagnetic in the bulk. In addition, many isomers with different spin magnetic moments are energetically nearly degenerate and this poses great challenges for theory to identify the true ground state of a transition metal cluster. Among these clusters, the *nd*-metal M_{13} species have received the most attention because of at least two reasons. First, the smallest icosahedral and cuboctahedral structures are composed of 13 atoms. Second, many transition metal clusters exhibit magic numbers at $n = 13$ in their time-of-flight mass spectra.[2] Several recent theoretical papers have recently been devoted to the computational study of clusters composed of 13 atoms in the whole range of the 3*d*-, 4*d*-, and 5*d*-metal series.[3–8] All these computations were performed using density functional theory (DFT) and effective core potentials with cores of different size.

While majority of the previous theoretical studies on M_{13} have been performed on the neutral species, experimental studies using mass-spectrometry and laser electron photodetachment techniques are performed on positively and negatively charged ions. To assess the accuracy of DFT methods, it is, therefore, necessary to study not only the neutral but also positively and negatively charged clusters. Our objective in this paper is to bridge this gap by carrying out a systematic and comprehensive study of the neutral and positively and negatively charged transition metal clusters. We have focused our study on the 13-atom clusters as we can not only compare our neutral structures with previous calculations, but also compare our results with experimental values of the vertical ionization energies (VIEs) of the neutral, vertical electron detachment energies from the anion, dissociation energies, and magnetic moments of the neutral and cationic species. This is achieved by performing all-electron DFT computations with generalized gradient approximation (GGA) on the M_{13}, $M_{13}{}^{-}$, and $M_{13}{}^{+}$ series with M from Sc to Zn. In order to obtain binding energies of atoms in the M_{13} and $M_{13}{}^{+}$ series, many of which were measured experimentally, we also considered the M_{12}, $M_{12}{}^{-}$, and $M_{12}{}^{+}$ series with M from Sc to Zn. These optimizations will provide additional theoretical values that can be compared with experimental data on the electron affinities and ionization energies.

The paper is organized as follows. First, we consider results of optimizations for each neutral M_{12} and M_{13} pair and their singly charged positive and negative ions. Second, we compute ionization energies and electron affinities for the lowest total energy states and compare these with experiment. Third, we compare our computed total spin magnetic moments with the experimental values available for Sc, Mn, Fe, Co, and Ni clusters. Finally, we compare our computed energies required to remove a single atom from M_{13} and $M_{13}{}^{+}$ with the corresponding experimental values, as well as with the bulk cohesive energies and binding energies of the M_2 dimers.

II. COMPUTATIONAL DETAILS

Our calculations are performed using DFT-GGA. The exchange-correlation functional is based on the Becke's

a)Email: gennady.gutsev@famu.edu

exchange[9] and Perdew-Wang correlation,[10] known as the BPW91 functional. The choice of this functional among many others is based on our previous assessment of this functional for 3*d*-metal oxides,[11–13] and the BPW91 stability in harmonic frequency calculations of closely spaced states of iron clusters.[14] The BPW91 functional is found to produce results which are quite close to those obtained using the coupled-cluster method with singles and doubles and non-iterative inclusion of triples [CCSD(T)][15] for $(TiO_2)_n$ clusters,[16] $(CrO_3)_n$ clusters,[17,18] and FeO_2.[19] Good agreement between the BPW91 results and experimental data was also obtained for $Cr_3O_8^-$.[20] The quality of new exchange-correlation functionals has been intensively tested using different databases[21] and the PW91 functional was found to have a good performance with respect to the best new functionals.[22] In particular, the PW91 method was found to have mean unsigned errors for transition metal atomization energies comparable to some of the most recent local and hybrid functionals.

The atomic orbitals are represented by the GAUSSIAN 6-311+G^* basis set [(15*s*11*p*6*d*1*f*/10*s*7*p*4*d*1*f*)[23,24] of the triple-ζ quality. Trial geometries were optimized without imposing symmetry constraints using the keyword NOSYMM in the GAUSSIAN 09 code.[25] For each neutral cluster, we tested a number of geometrical structures available in the literature as well as those generated from the layered structures N_1-N_2-...N_k, where N_i is number of atoms in the *i*th layer, with interatomic distances typical for a given atom. Pre-optimizations of states with trial structures were performed using a smaller 6-311G^* basis set. In optimizations of the ions, we started with the geometrical structures found for the neutral lowest total energy state as well as the energetically closest isomers.

For a given geometrical structure, all possible spin multiplicities were tried in order to determine the total spin of the lowest total energy state. The convergence threshold for total energy was set to 10^{-8} eV and the force threshold was set to 10^{-3} eV/Å. Each geometry optimization was followed by harmonic frequency computations in order to confirm the stationary character of the state obtained. If geometry optimization led to a transition state, further optimizations following the imaginary frequency modes were performed until all imaginary frequencies are eliminated. Local spin magnetic moments on atoms which are identified with the excess spin densities on atoms are obtained using the Natural Atomic Orbital (NAO)[26] population analysis.

III. RESULTS AND DISCUSSION

A. Geometrical structures

1. Sc_{13} and Sc_{12}

Following the Stern-Gerlach measurements[27] of a total magnetic moment of neutral Sc_n clusters, several theoretical studies[28–33] using both all-electron and effective core potential (ECP) methods were performed with the aim to reproduce the experimental values. All theoretical studies including the present work found the lowest total energy state of Sc_{13} to possess nearly icosahedral geometry (see Fig. 1) and a total spin magnetic moment of 19 μ_B which is very far from

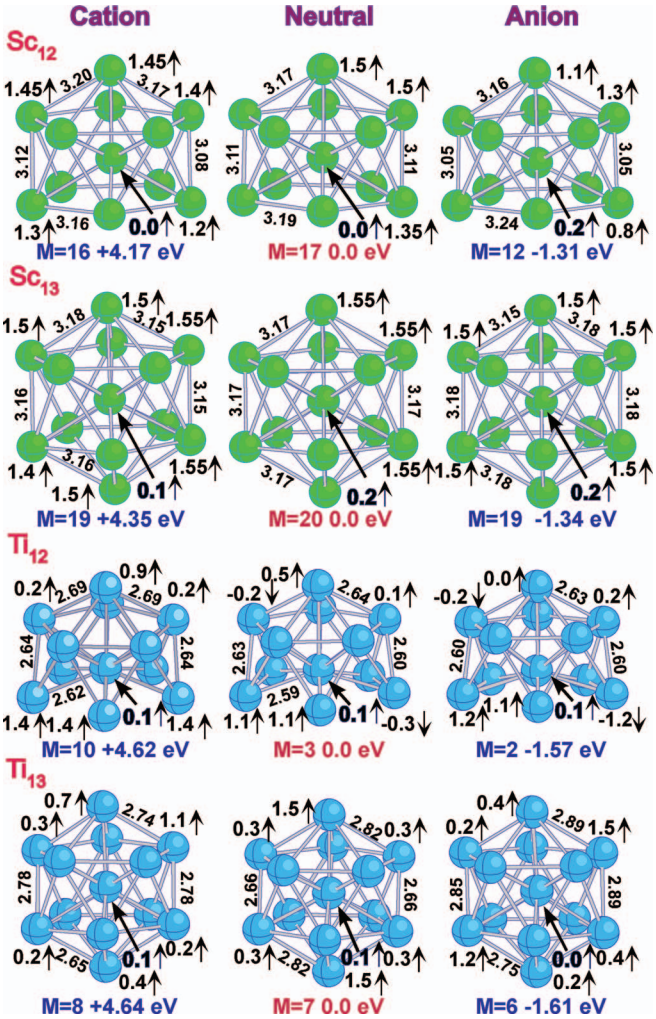

FIG. 1. Geometrical structure and local spin magnetic moments in the lowest total energy states of the neutral and charged Sc_n and Ti_n clusters, $n = 12$ and 13. Bond lengths are in Angstroms, magnetic moments are in Bohr magnetons, and M is the spin multiplicity $2S + 1$.

the experimental value of 6.0 ± 0.2 μ_B. According to the results of our optimizations performed without imposing symmetry constraints, the closest in total energy state with a total spin magnetic moment of 17 μ_B is higher in total energy by 0.27 eV. The states with total spin magnetic moments of 5 μ_B and 7 μ_B which are close to the value obtained in the experiment are higher in total energy by 1.71 eV and 1.62 eV, respectively.

According to the results of our NAO analysis, the valence population at the central Sc atom is $4s^{0.43}3d^{4.67}4p^{1.55}4d^{0.21}$ and corresponds to the AO occupation by 6.86 electrons. That is, the central atom carries a negative charge of $-3.86e$. All surface atoms possess the valence population of $4s^{0.41}3d^{1.83}4p^{0.46}$, composed of the α-$4s^{0.26}3d^{1.57}4p^{0.29}$ and β-$4s^{0.15}3d^{0.26}4p^{0.17}$ constituents, which corresponds to the charge of $+0.3e$ per atom. Note, that there is no exact charge balance because of neglected small contributions from AOs with higher quantum numbers.

Reoptimizations of this Sc_{13} state obtained without symmetry constraints with imposing I_h symmetry constrains resolved by symmetry the valence molecular orbitals

(MO) but left unresolved by symmetry MOs composed of the core AOs. If I_h symmetry is reduced to T_h, then one obtains all symmetry resolved MOs corresponding to the $^{20}A_u$ state. This state is degenerate in total energy with the state obtained without symmetry constraints whose NAO populations are given above. However, a drastic change in NAO population is observed in the $^{20}A_u$ state. The effective electronic configuration of the central atom in this state is $4s^{0.69}3d^{5.47}4p^{0.05}4d^{0.14}$, which corresponds to a charge of $-3.35e$. All other atoms possess the $4s^{0.72}3d^{1.92}4p^{0.03}4d^{0.08}$ effective electronic configurations corresponding to a charge of $+0.24e$. That is, there is almost no $4s \rightarrow 4p$ promotion in the $^{20}A_u$ state. Apparently, there is a strong competition between $4s$ promotion to vacant $3d$ and $4p$ AOs.

The lowest total energy state of Sc_{12} possesses a slightly distorted icosahedral geometry with a total spin magnetic moment of 16 μ_B and is nearly degenerate in total energy with the states whose total spin magnetic moments are 14 μ_B (+0.05 eV), 12 μ_B (+0.06 eV), and 6 μ_B (+0.10 eV). A state of Sc_{12} with a total spin magnetic moment of 2 μ_B possesses a cylindrical geometrical structure which is produced from that presented in Fig. 1 by shifting the central and apex atoms to the centers of the cylinder planes formed by two five-membered rings. We found that the lowest energy state with this geometry is the state with a total spin magnetic moment of 6 μ_B which is higher in total energy by 0.15 eV than the lowest total energy state with a total spin magnetic moment of 16 μ_B. The charge on the central Sc atom reduces to −3.14 e and the $4p$ occupation of all atoms is nearly depleted.

Both detachment and attachment of an electron from/to Sc_{12} and Sc_{13} do result in minor changes in the geometrical structures of the neutrals. If one accepts a one-electron model where an electron detaches/attaches from/to a spin-up or spin-down occupied/virtual orbital without significant reconstruction of the rest of orbitals, then a total spin magnetic moment of a charged cluster would change from its neutral value by ±1.0 μ_B. This is the case for the Sc_{12}–Sc_{12}^+, Sc_{13}–Sc_{13}^-, and Sc_{13}–Sc_{13}^+ pairs but not for the Sc_{12}–Sc_{12}^- pair, where the change is 5.0 μ_B. The states of Sc_{12}^- that do satisfy the one-electron rule are higher in total energy by +0.02 eV (a total spin magnetic moment of 15 μ_B) and +0.05 eV (a total spin magnetic moment of 17 μ_B). It will be interesting to compare the magnetic moments of Sc_{12}^+ and Sc_{13}^+ with experiments when available.

2. Ti_{13} and Ti_{12}

Geometrical structures found for the lowest total energy states of the neutral and charged Ti_{12} and Ti_{13} clusters are displayed in Fig. 1. The geometrical structure of the lowest total state of neutral Ti_{13} is found to be a slightly distorted icosahedron (ICO) in agreement with the previous assignments.[34–43] Our value of 6 μ_B for the total spin magnetic moment of Ti_{13} is also in agreement with the result of a recent study.[44] The effective electron configuration of the central Ti atom in Ti_{13} is $4s^{0.40}3d^{4.41}4p^{1.38}4d^{0.19}$, which means that the central atom carries a negative charge of $-2.4e$. The effective electron configurations of two apex atoms are $4s^{0.35}3d^{2.99}4p^{0.36}4d^{0.02}$ and all other atoms have the $4s^{0.39}3d^{3.06}4p^{0.40}4d^{0.02}$ configuration.

The geometrical structure of the lowest total energy state of Ti_{12} is formed from the Ti_{13} geometry by the removal of an apex atom in agreement with the results of previous studies. As is seen from Fig. 1, this removal causes serious changes in the local spin magnetic moments with respect to those in Ti_{13} and the rupture of bonds in the bottom pentagon ring. Our value of a total spin magnetic moment is 2 μ_B, which is the same as that obtained at the BLYP level by Medina *et al.*[44]

The lowest total energy states of Ti_{13}^+ and Ti_{13}^- possess strongly distorted icosahedral geometrical configurations with large variations in the local spin magnetic moment values. Total spin magnetic moments of Ti_{13}^+ and Ti_{13}^- are 7 μ_B and 5 μ_B, respectively, which is in agreement with the results of a previous study.[45] Whereas the single-electron rule is valid for the electron attachment and detachment processes of Ti_{13}, it is not so for Ti_{12} because its cation has a total spin magnetic moment of 9 μ_B. In order to make sure that this is not an artifact of the basis set, we recomputed the cation states using the 6-311+G(3df) basis set (15s11p6d3f1g/10s7p4d3f1g). The results of optimizations with the 6-311+G* and 6-311+G(3df) basis sets for the states with total spin magnetic moments from 1 μ_B to 11 μ_B are presented in Fig. 2. As is seen, the "skirt" bonds are all broken in the states with total spin magnetic moments larger than 3 μ_B and the basis extension does not lead to the change in the order of total energies of the states. The state with a total spin magnetic moment of 3 μ_B, which satisfies the one-electron rule, is higher in total energy by 0.01–0.02 eV.

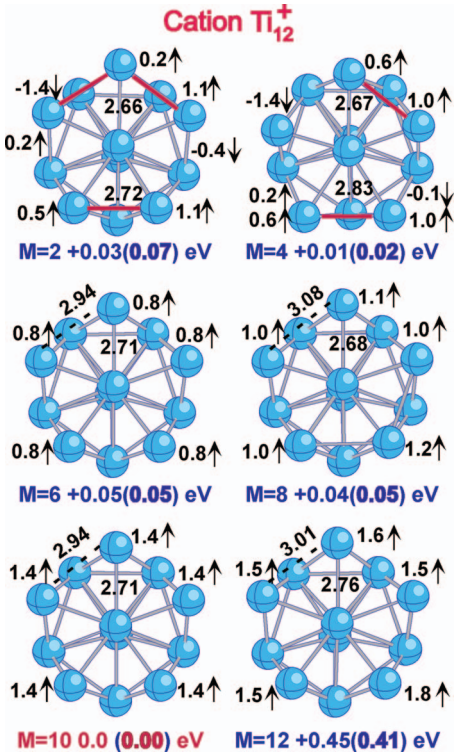

FIG. 2. Geometrical structures of the Ti_{12}^+ isomers corresponding to the lowest total energy states with the spin multiplicity from 2 to 12. Bond lengths are in Angstroms, magnetic moments are in Bohr magnetons, and M is for the spin multiplicity $2S + 1$. The values in parentheses are obtained using the 6-311+G(3df) basis set.

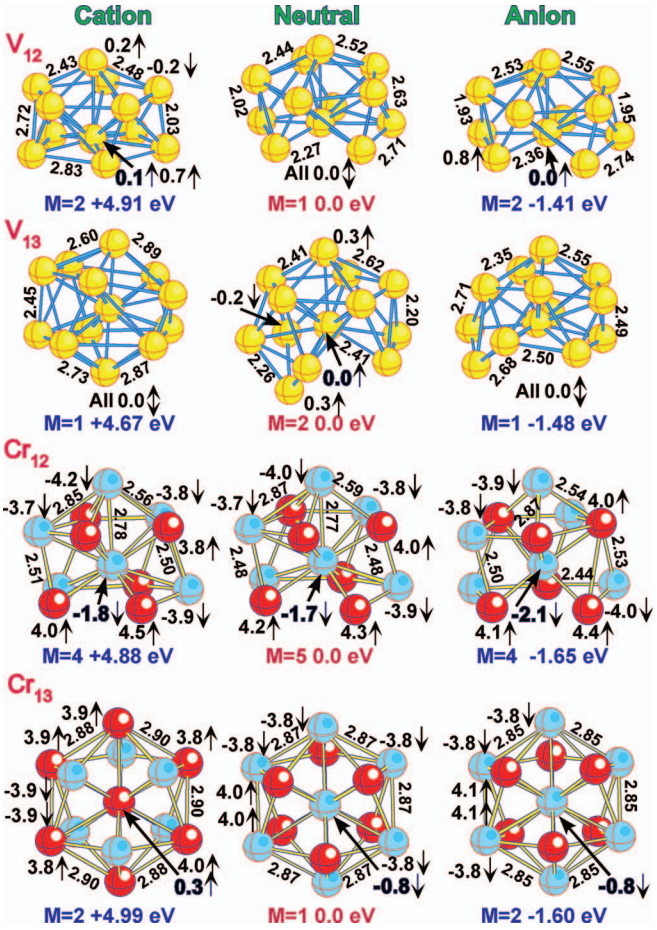

FIG. 3. Geometrical structure and local spin magnetic moments in the lowest total energy states of the neutral and charged V_n and Cr_n clusters, $n = 12$ and 13. Bond lengths are in Angstroms, magnetic moments are in Bohr magnetons, and $M = 2S + 1$. In the Cr_n series, the red and blue colors are used to mark atoms with the local spin-up and spin-down magnetic moments, respectively.

3. V_{13} and V_{12}

The geometrical structures of the lowest total energy states found for the neutral and charged V_{13} and V_{12} clusters are shown in Fig. 3. The V_{13} cluster has a doublet lowest total energy state with a strongly distorted I_h geometry in agreement with the previous studies.[46,47] Our structure is open in the bottom where the bonds between the atoms are broken. However, the determination of the lowest total energy state is difficult because we found eight doublet and quartet states whose difference in total energy with respect to the lowest energy state given in Fig. 3 is less than 0.1 eV. Both V_{13}^+ and V_{13}^- possess the singlet lowest total energy states with distorted icosahedral geometrical configurations. All V_{12} species are found to possess the bell-shaped geometrical structures in their lowest total energy states. An icosahedral cage structure was previously found[48] for the lowest total energy doublet state of the V_{12}^+ cation. According to the results of our BPW91/6-311+G* computations, the V_{12}^+ doublet state with such a cage structure is above the state whose geometrical structure is given in Fig. 3 by only 0.007 eV. Reoptimizations at the BPW91/6-311+$G(3df)$ level resulted in a larger total energy difference of +0.028 eV; therefore, we accept the structure in Fig. 3 as corresponding to the lowest total energy state of V_{12}^+. No violation of the one-electron rule is found for either V_{12} or V_{13}.

4. Cr_{13} and Cr_{12}

According to the results of previous computations,[49,50] the lowest total energy state of Cr_{13} is either a cubo-octahedral or an icosahedron type structure.[7] The geometrical structure we found for the lowest total energy antiferromagnetic singlet state of Cr_{13} (see Fig. 3) has a similar shape and the same arrangement of atoms carrying spin-up and spin-down magnetic moments as found previously in Ref. 7. One bond between the atoms possessing the spin-up magnetic moments is broken in the upper and bottom pentagons. Both attachment and detachment of an electron do not lead to the change in the geometrical structure of the neutral lowest total energy state.

The lowest total energy states of Cr_{12} and its ions possess the bell-type geometrical structures with a broken bond in the bottom pentagon (see Fig. 3). The lowest total energy state of Cr_{12} possesses a total spin magnetic moment of 4 μ_B whereas both the ions have the same total spin magnetic moment of 3 μ_B in accordance with the one-electron rule. The neutral singlet, triplet, and nonet states are higher in total energy by only 0.07 eV, 0.01 eV, and 0.02 eV, respectively. The doublet state of the Cr_{12}^- anion is only marginally higher in total energy by 0.01 eV than its quartet state, whereas the doublet state of the cation is higher in total energy by 0.09 eV than the cation quartet state. The sextet states of both anion and cation are higher than their quartet states by 0.14 eV and 0.40 eV, respectively.

5. Mn_{13} and Mn_{12}

The lowest total energy state of Mn_{13} is an antiferromagnetic quartet and possesses a slightly distorted icosahedral geometrical structure.[51–55] The Mn_{13}^+ and Mn_{13}^- ions do possess similar geometrical structures (see Fig. 4) as their neutral parent with total magnetic moments of 2 μ_B and 4 μ_B, respectively.[56,57] The NAO effective electronic configuration of the central Mn atom is $3d^{7.53}4s^{0.97}4p^{0.15}$ and corresponds to the charge of $+1.65e$.

There is no agreement between our results and previous studies on a total spin magnetic moment of the Mn_{12} cluster. Whereas we obtained the same arrangement of local spin magnetic moments as obtained by Bobadova-Parvanova *et al.*,[58] our total spin magnetic moment is smaller by 4 μ_B. Kabir *et al.*[59] obtained a total spin magnetic moment of 16 μ_B for Mn_{12}, i.e., twice as large as our value. Because of various possible arrangements of spin-up and spin-down local spin magnetic moments, Mn_{12} and its ions possess a plenty of states, many of which are close in total energy. We found dozens of states, which are within 0.1 eV in total energy from the lowest total energy state in both neutral and charged Mn_{12} clusters. Therefore, the assignment of the ground state for these clusters is challenging. The one-electron rule is valid for the $n = 13$ series but not for the $n = 12$ series.

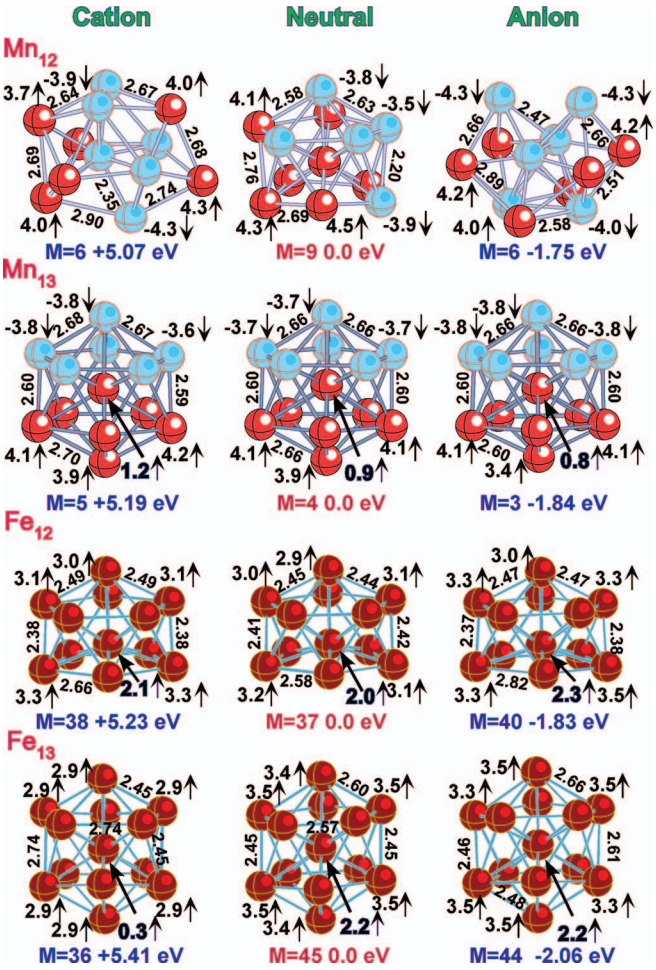

FIG. 4. Geometrical structure and local spin magnetic moments in the lowest total energy states of the neutral and charged Mn_n and Fe_n clusters, $n = 12$ and 13. Bond lengths are in Angstroms, magnetic moments are in Bohr magnetons, and $M = 2S + 1$. In the Mn_n series, the red and blue colors are used to mark atoms with the local spin-up and spin-down magnetic moments, respectively.

6. Fe_{13} and Fe_{12}

The ground state geometries of the neutral and charged Fe_{12} and Fe_{13} clusters are displayed in the bottom panels of Fig. 4. The iron clusters possess the largest total spin magnetic moments in the Sc–Zn series although the largest local spin magnetic moments belong to the Mn clusters. The lowest total energy states of the Fe_{13} and Fe_{13}^- clusters possess Jahn-Teller distorted icosahedral geometries,[60–69] whereas the lowest total energy state of Fe_{13}^+ has T_h symmetry.[70] Note that the neutral Fe_{13} state possesses T_h symmetry at $2S + 1 = 47$ whereas the lowest total energy state of Fe_{13} has the spin multiplicity of 45. The lowest total energy states of Fe_{12} and its ions possess similar geometrical structures of an icosahedron with an apex atom removed. The one-electron rule is not valid for either Fe_{13} or Fe_{12}. An especially drastic change in the total spin magnetic moment is observed[71] for Fe_{13}^+, whose total spin magnetic moment is smaller than that of its neutral parent by 9 μ_B. The results of our computations are in agreement with this finding. A detailed discussion on the structure and peculiarities of the neutral and singly charged iron clusters Fe_n ($n = 7$–20) can be found in our recent paper.[72]

7. Co_{13} and Co_{12}

The geometry of the lowest total energy state of Co_{13} obtained in a number of studies corresponds to a slightly distorted ICO[73–79] whereas other studies[80–82] predicted the Co_{13} geometry to be a hexagonal bilayer (HBL). These studies have shown that the values of the local spin magnetic moments depend strongly on the geometrical structure found for the lowest total energy state as well as on the method and basis set used.[83] Lv *et al.*[84] performed all-electron DFT optimizations for two states of Co_{13} possessing the ICO and HBL structures in the range of total spin magnetic moments from 13 μ_B to 33 μ_B. They found the absolute minimum in total energy to correspond to a state with the HBL geometry and a total spin magnetic moment of 27 μ_B. A state with an ICO geometry and a total spin magnetic moment of 31 μ_B was found to correspond to a local minimum, which is below in total energy than the HBL state with this total spin magnetic moment. We found the HBL state of Co_{13} to have the lowest total energy (Fig. 5). Our search for the lowest total energy state of Co_{13} led to 7 states with the spin multiplicity of 28, including a state with a distorted ICO geometry as obtained

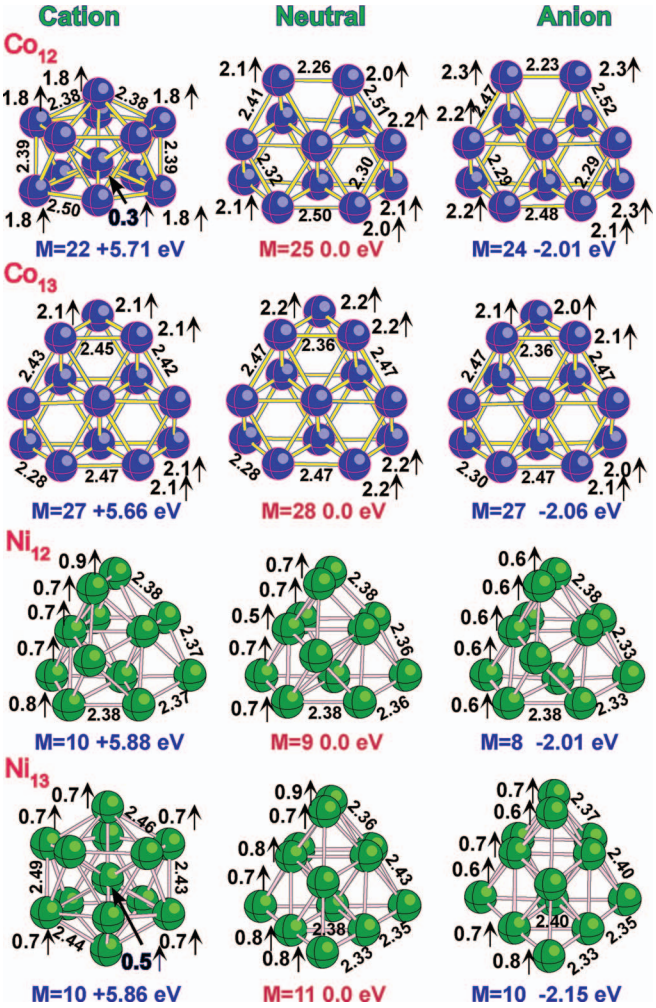

FIG. 5. Geometrical structure and local spin magnetic moments in the lowest total energy states of the neutral and charged Co_n and Ni_n clusters, $n = 12$ and 13. Bond lengths are in Angstroms, magnetic moments are in Bohr magnetons, and $M = 2S + 1$.

by Datta *et al.*,[85] whose total energies are placed between those of states with the HBL and ICO geometrical structures. The Co_{13}^- and Co_{13}^+ ions also possess the HBL geometrical structures and obey the one-electron rule.

Both Co_{12} and Co_{12}^- possess geometrical configurations obtained from those of Co_{13} and Co_{13}^- via the removal of the top atom (see Fig. 5). Extensive optimizations of Co_{12}^+ yielded a state with an ICO geometry and a total spin magnetic moment of 21 μ_B for the lowest total energy state. The geometrical configurations of Co_{12}^+ states are also probed by removing the top or a bottom atom from the HBL configuration. This yielded a state with a total spin magnetic moment of 23 μ_B which is only 0.03 eV higher in total energy than the lowest total energy state. The violation of the one-electron rule for the Co_{12}–Co_{12}^+ pair can be related to the change in the geometrical topology.

8. Ni_{13} and Ni_{12} clusters

An ICO structure and the magnetic moment of 8 μ_B was found for the lowest total energy state of Ni_{13} in the majority of previous studies.[86–101] However, two recent papers[7,102] have obtained non-icosahedral structures for the lowest total energy state of Ni_{13}, which correspond to structures **I** and **IV** shown in Fig. 6, respectively, and a total spin magnetic moment of 10 μ_B. The computations were performed using the Perdew-Burke-Ernzerhof (PBE) functional[103] in both papers.

In order to gain insight into the dependence of the optimization results on the exchange-correlation functional and basis set used, we performed optimizations of four isomers presented in Fig. 6 using the 6-311+*G** and extended 6-311+*G*(3*df*) basis sets and four different methods, namely, the BPW91, PBE, TPSS,[104] and M06-L[105] methods. The results of computations are presented in Table I. As is seen, all four methods predict the icosahedral geometrical structure and $2S + 1 = 9$ for the lowest total energy state of Ni_{13} independent of the basis set used except for the BPW91 method. The electronic energy of the $2S + 1 = 11$ state with geometrical configuration **I** is lower than that of the $2S + 1 = 9$ state with geometrical configuration **II** by 0.027 eV at the BPW91/6-311+G* level. The addition of zero-point vibrational energies (ZPVE) to the electronic energies makes the latter state to be marginally lower in total energy. The basis extension leads to the decreasing differences in total energies obtained using the PBE, TPSS, and M06-L methods, whereas the $2S + 1 = 11$ state with geometrical configuration **I** becomes the lowest total energy state at the BPW91/6-311+*G*(3*df*) level. Taking into account the trend toward decreasing the **I**–**II** difference in total energy when the basis set increases, we assign geometrical configuration **I** and $2S + 1 = 11$ as corresponding to the lowest total energy state of Ni_{13}.

TABLE I. Relative total energies of the Ni_{13} isomers with the geometries **I**–**IV** displayed in Fig. 6. All values are in eV.

		Basis 6-311+G*			
Isomer	$2S+1$	BPW91	PBE	TPSS	M06-L
I	9	0.27	0.37	0.52	1.16
	11	0.005	0.09	0.23	0.57
II	9	0.00	0.00	0.00	0.00
	11	0.49	0.48	0.37	0.15
III	9	0.20	0.28	0.43	1.06
	11	0.08	0.14	0.23	0.50
IV	9	0.18	0.25	0.38	1.05
	11	0.11	0.17	0.27	0.66
		Basis 6-311+*G*(3df)			
I	11	0.00	0.02	0.14	0.47
II	9	0.06	0.00	0.00	0.00

An anion state with $2S + 1 = 10$ and geometrical configuration **I** presented in Fig. 5 is energetically lower by 0.09 eV than the state with $2S + 1 = 8$ and geometrical configuration **II**. The latter state possesses the smallest total energy among the states with icosahedral geometries and different spin multiplicities. A state of the cation with $2S + 1 = 10$ and an icosahedral geometrical structure (presented in Fig. 5) is lower in total energy by 0.04 eV than the state with $2S + 1 = 12$ and geometrical configuration **I**. It is worth noting that the cation states possessing geometrical configurations **I**–**IV** and total spin magnetic moments of 9 μ_B and 11 μ_B, are all within less than 0.1 eV in total energy.

All three clusters Ni_{12}, Ni_{12}^+, and Ni_{12}^- possess similar geometrical configurations obtained from **I** by the removal of the front atom in the base (see Fig. 5), and all of them possess isomers whose total energies are within 0.1 eV from the total energy of the corresponding lowest total energy states. No violation of the one-electron rule is observed for these nickel clusters.

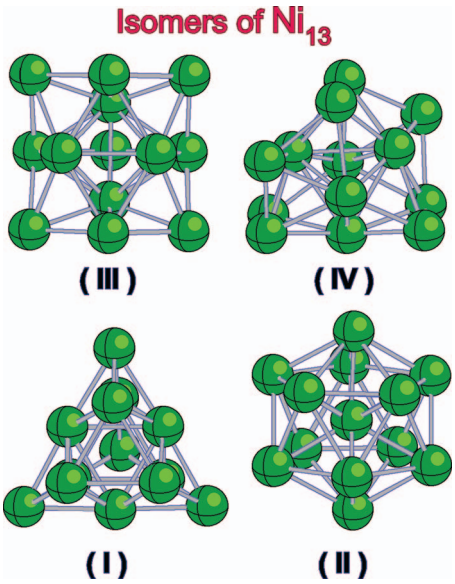

FIG. 6. Geometrical structures of four isomers, which are candidates for the geometrical structures of the lowest total energy state of Ni_{13}.

9. Cu_{13} and Cu_{12}

A number of different geometrical structures have previously been assigned for the lowest total energy states of the neutral Cu_{13} and Cu_{12} clusters.[7,106–114] Somewhat

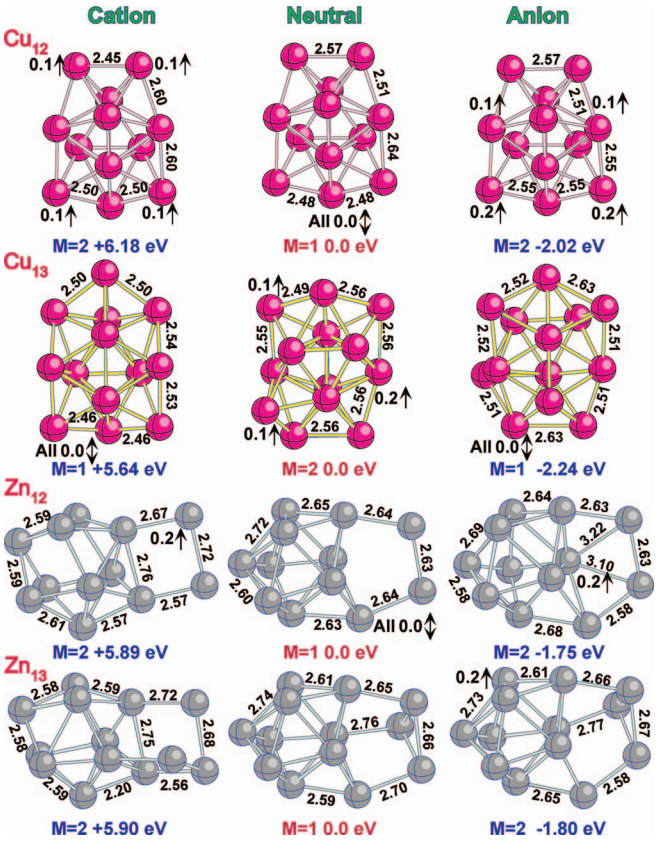

FIG. 7. Geometrical structure and local spin magnetic moments in the lowest total energy states of the neutral and charged Cu_n and Zn_n clusters, $n = 12$ and 13. Bond lengths are in Angstroms, magnetic moments are in Bohr magnetons, and $M = 2S + 1$.

different geometrical structures were also obtained for the Cu_{13}^+ and Cu_{12}^+ cations[113,115] and the Cu_{13}^- and Cu_{12}^- anions.[113,116,117] Our search for the geometrical structure of the lowest total energy state of Cu_{13} resulted in the structure shown in Fig. 7 which is similar to that found in the most recent papers cited above. The similar structures as found recently are obtained for the Cu_{13} and Cu_{12} ions (see Fig. 7) in the present work as well. There is no violation of the one-electron rule in the Cu_{13} and Cu_{12} series.

10. Zn_{13} and Zn_{12}

The geometrical configurations of the lowest total energy states of the neutral and charged Zn_{13} and Zn_{12} clusters are displayed in Fig. 7. Previously computed[7,118,119] geometrical structures for Zn_{13} and Zn_{12} are similar to those presented in the figure. Both attachment and detachment of an electron to/from either Zn_{13} or Zn_{12} result in substantial reconstructions of the neutral geometries except for Zn_{13}^-. As in the preceding case, there is no violation of the one-electron rule.

B. Ionization energies and electron affinities

In order to assess the quality of the present computations on the M_{12} and M_{13} neutrals and their ions, we begin with comparing our values of ionization energies with experiment. We computed the adiabatic ionization energy of a neutral according to the equation

$$IE_{\rm ad}(M_n) = E_{\rm tot}^{\rm el}(M_n^+) + {\rm ZPVE}(M_n^+) - \left[E_{\rm tot}^{\rm el}(M_n) + {\rm ZPVE}(M_n)\right], \quad (1)$$

where $E_{\rm tot}^{\rm el}(M_n)$ and $E_{\rm tot}^{\rm el}(M_n^+)$ are the total electronic energies of M_n and M_n^+, respectively, and ZPVE is the zero-point vibrational energy computed in the harmonic approximation.

The VIE of a neutral are computed at the geometry of the neutral lowest total energy state for two different electron detachment channels corresponding to the final cation states whose spin multiplicities differ from the spin multiplicity of the neutral parent by ± 1. The corresponding formula for the VIE is given by the expression

$$VIE_{\pm}(M_n) = E_{\rm tot}^{\rm el}(M_n^+, (2S+1) \pm 1) - E_{\rm tot}^{\rm el}(M_n, 2S+1). \quad (2)$$

The computed values are compared with experiment in Table II. Note that the experimental values are obtained from mass-spectrometry experiments and correspond to the vertical electron detachment processes. As is seen, the differences between the theoretical and experimental values do not exceed 0.2 eV when the experimental uncertainty bars are taken into account except for Mn_{12}.

Next, we compare the results of our computations for the M_{12}^- and M_{13}^- anions with experiment. The adiabatic energy of an electron attachment to a neutral corresponds to the adiabatic electron affinity ($EA_{\rm ad}$) of the neutral and is computed as

$$EA_{\rm ad}(M_n) = E_{\rm tot}^{\rm el}(M_n) + {\rm ZPVE}(M_n) - \left[E_{\rm tot}^{\rm el}(M_n^-) + {\rm ZPVE}(M_n^-)\right]. \quad (3)$$

The vertical electron detachment energies of the anion are computed at the geometry of the anion lowest total energy state according to the equation

$$VDE_{\pm}(M_n^-) = E_{\rm tot}^{\rm el}(M_n, 2{\rm S}+1) - E_{\rm tot}^{\rm el}(M_n^-, (2{\rm S}+1) \pm 1). \quad (4)$$

Experimental laser electron photodetachment spectra correspond to the vertical electron detachment processes. Experimental energies corresponding to the 0-0 electronic transitions (from the zero vibrational level of an anion to that of the neutral) provide good estimates for the adiabatic energies if the geometrical relaxation of the final neutral state is relatively small. Occasionally, it is difficult to recover the feature corresponding to the 0-0 transition in the spectra. In Table III, which compares the computed and experimental values, the experimental entries without uncertainty bars correspond to approximate values obtained from the spectra without visibly resolved 0-0 transitions. As is seen from the table, our computed values are again within 0.1 eV from the corresponding experimental values when the experimental uncertainty bars are taken into account. Because our computed values for the ionization energies and electron affinities are in good agreement with experiment, we conclude that the lowest total energy states found for the M_{12} and M_{13} neutrals and their ions are to be close to the true ground states.

TABLE II. Comparison of the BPW91/6-311+G* values of the vertical (IE_{vert}) and adiabatic ionization energies (IE_{ad}) for the neutral M_{12} and M_{13} series with experiment. All values are in eV.

	M_{12} series									
	Sc_{12}	Ti_{12}	V_{12}	Cr_{12}	Mn_{12}	Fe_{12}	Co_{12}	Ni_{12}	Cu_{12}	Zn_{12}
$M = 2S + 1$	17	3	1	5	9	37	25	9	1	1
$IE_{vert}(M + 1)$	4.59	4.70	4.94	5.31	5.29	5.33	5.79	5.91	6.24	6.33
$IE_{vert}(M - 1)$	4.20	4.72		4.90	5.31	5.27	5.80	6.26		
IE_{ad}	4.17	4.62	4.91	4.88	5.15	5.23	5.71	5.88	6.18	5.89
Exp.			4.95 ± 0.05[a]	5.32 ± 0.05[b]	4.88[c]	5.52 ± 0.05[d] 5.42 ± 0.16[e]	5.70 ± 0.05[f] 5.64 ± 0.06[e]	5.90[g] 5.77± 0.21[e]	6.31 ± 0.1[h]	
	M_{13} series									
	Sc_{13}	Ti_{13}	V_{13}	Cr_{13}	Mn_{13}	Fe_{13}	Co_{13}	Ni_{13}	Cu_{13}	Zn_{13}
$M = 2S + 1$	20	7	2	1	4	45	28	11	2	1
$IE_{vert}(M + 1)$	4.78	4.70	4.89	5.36	5.26	5.89	6.08	5.94	6.38	6.20
$IE_{vert}(M - 1)$	4.42	4.68	4.76		5.39	5.62	5.67	6.05	5.78	
IE_{ad}	4.35	4.64	4.67	4.99	5.19	5.41	5.66	5.86	5.64	5.90
Exp.			4.93 ± 0.05[a]	5.18 ± 0.05[b]	5.30[c]	5.61 ± 0.05[d] 5.76 ± 0.18[e]	5.74 ± 0.05[f] 5.84 ± 0.26[e]	5.88[g] 5.77 ± 0.19[e]	5.66 ± 0.1[h]	

[a]See Ref. 136.
[b]See Ref. 137.
[c]See Ref. 138.
[d]See Refs. 139 and 140.
[e]See Ref. 141.
[f]See Ref. 142.
[g]See Ref. 143.
[h]See Ref. 144.

C. Magnetic moments

Total magnetic moments of *neutral* transition metal clusters were measured using Stern-Gerlach experiments for Sc_n, n = 5–20,[27] for Cr_n, n = 20–133,[120] Mn_n,[121] Fe_n, n = 10–25,[122] Fe_n, n = 25–700,[123] Co_n, n = 20–200,[124] n = 12–200,[125] n = 7–32,[126] n = 13–200,[127] Ni_n, n = 25–700,[128] n = 5–740,[129] and *cationic* transition metal clusters using X-ray magnetic circular dichroism (XMCD) experiments for Fe_n^+, n = 3–20,[71] and Co_n^+, n = 8–22.[130] Two branches of total magnetic moments per atom were found for Cr_n clusters[120] as well as for Fe_n and Co_n clusters.[131]

The total magnetic moment in the Russel-Saunders scheme is defined as $\boldsymbol{\mu} = (2\mathbf{S} + \mathbf{L})\ \mu_B$, where μ_B is the Bohr magneton, and **L** and **S** are the total angular and spin moments, respectively. In the Heisenberg model, one neglects the **L** contribution and defines $\mu = g_e \mu_B S$ where the

TABLE III. Vertical ionization energies (IE_{vert}) of the lowest total energy states in the M_{12}^- and M_{13}^- series and adiabatic electron affinities (EA_{ad}) of the corresponding neutral parents. All values are in eV.

	Sc_{12}^-	Ti_{12}^-	V_{12}^-	Cr_{12}^-	Mn_{12}^-	Fe_{12}^-	Co_{12}^-	Ni_{12}^-	Cu_{12}^-	Zn_{12}^-
$M = 2S + 1$	12	2	2	4	6	40	26	8	2	2
$IE_{vert}(M + 1)$	1.38	1.61	1.64	1.67	1.97	2.33	2.26	2.03	2.72	2.96
$IE_{vert}(M - 1)$	1.49	1.59	1.60	1.67	1.92	1.87	2.04	2.41	2.08	1.89
EA_{ad}	1.31	1.57	1.41	1.65	1.57	1.83	2.01	2.01	2.02	1.75
Exp		1.71 ± 0.05[a]	1.48[b]	1.8[c]		2.14 ± 0.06[d]	2.2[e]	2.09 ± 0.05[f]	2.12 ± 0.05[g]	2.0[h]
	Sc_{13}^-	Ti_{13}^-	V_{13}^-	Cr_{13}^-	Mn_{13}^-	Fe_{13}^-	Co_{13}^-	Ni_{13}^-	Cu_{13}^-	Zn_{13}^-
$M = 2S + 1$	19	6	1	2	3	44	27	10	1	2
$IE_{vert}(M + 1)$	1.35	1.67	1.58	2.20	1.92	2.22	2.08	2.17	2.28	3.01
$IE_{vert}(M - 1)$	1.63	1.71		1.62	2.12	2.12	2.20	2.43		1.95
EA_{ad}	1.34	1.61	1.48	1.60	1.84	2.06	2.06	2.15	2.24	1.80
Exp		1.87 ± 0.05[a]	1.5[b]	1.8[c]	2.2 ± 0.1[i] 1.9 ± 0.1[i]	2.24 ± 0.06[d]	2.3[e]	2.16 ± 0.05[f]	2.33 ± 0.05[g]	1.9[h]

[a]See Ref. 145.
[b]See Refs. 146 and 147.
[c]See Ref. 148.
[d]See Refs. 149 and 150.
[e]See Ref. 151.
[f]See Ref. 152.
[g]See Refs. 153–155.
[h]See Ref. 156.
[i]See Ref. 56; the values do correspond to the IE_{vert} and the EA_{ad}, respectively.

TABLE IV. Comparison of the calculated total spin magnetic moments per atom with experiment for the M_{12} and M_{13} species.[a]

	Sc_{12}	Mn_{12}	Fe_{12}	Fe_{12}^+	Co_{12}	Co_{12}^+	Ni_{12}
Theo	1.33	0.67	3.00	3.08	2.00	1.75	0.67
Exper	0.18 ± 0.02[b]	1.08 ± 0.2[c]	5.2[d]	3.41 ± 0.50[e] 3.50 ± 0.51[e]	2.21 ± 0.01[f] 2.26 ± 0.08[g]	2.5[h] 3.3 ± 0.2[h]	1.15[i]
	Sc_{13}	Mn_{13}	Fe_{13}	Fe_{13}^+	Co_{13}	Co_{13}^+	Ni_{13}
Theo	1.46	0.23	3.38	2.69	2.08	2.00	0.77
Exper	0.46 ± 0.02[b]	0.56 ± 0.1[c]	2.5 ± 0.1[d]	2.44 ± 0.38[e] 2.63 ± 0.41[e]	2.00 ± 0.06[f] 2.30 ± 0.07[g] 3.91 ± 0.60[j]	2.05[h] 2.65 ± 0.2[h]	0.95[i]

[a]All values are in Bohr magnetons.
[b]See Ref. 27.
[c]See Ref. 121.
[d]See Ref. 122.
[e]See Ref. 71, the first value corresponds to a total spin magnetic per atom and the second value corresponds to a total magnetic per atom.
[f]See Ref. 125.
[g]See Ref. 126.
[h]See Ref. 130; the first value corresponds to a total spin magnetic moment per atom and the second value corresponds to a total magnetic moment per atom.
[i]See Ref. 129.
[j]See Ref. 127.

gyromagnetic ratio g_e is 2.0023. In the XMCD experiments performed for the Fe_n^+ and Co_n^+, the contributions from both moments were separated whereas that was not possible in the Stern-Gerlach experiments. It was found for the iron cation series that "the orbital magnetic moment is strongly quenched and reduced to 5%–25% of its atomic value,"[71] whereas "an exceptionally strong enhancement of the orbital moment" was reported for the cobalt cation series.[130] Theoretical estimates[132] of the angular moment contributions for small Ni_n clusters predicted these contributions to account for 20%–40% of total magnetic moments of the nickel clusters. We consider the total spin magnetic moment, $M = 2S\ \mu_B$, to be equal to $[n_\alpha - n_\beta]\ \mu_B$, where n_α and n_β are the numbers of the majority spin and minority spin electrons, respectively.

Our values are compared to the experimental values of total magnetic moments and total spin magnetic moments obtained for the iron and cobalt cations in Table IV. As is seen, there is good agreement for the iron cations, neutral cobalt species, and Co_{13}^+, whereas large differences remain in other cases. An especially large difference is obtained for Fe_{12} where the experimental value of 5.2 μ_B is larger than our computed value by 2.2 μ_B. The possibility that the difference is due to a large orbital angular momentum contribution is discounted by the fact that such a contribution is small in the case of Fe_{12}^+.

Total spin magnetic moments per atom computed in this work are presented in Figs. 8 and 9 for the M_{12} and M_{13} series, respectively. The largest dependence on the charge is observed in the beginning of the M_{12} series, whereas small variations in the middle-to-end series are consistent with the one-electron rule. There is no visible dependence on the charge in the M_{13} series except for Fe_{13}^+ whose total spin magnetic moment per atom is appreciably lower than that of Fe_{13} or Fe_{13}^-.

D. Thermodynamic stability

Experimental values obtained from mass-spectrometry measurements and our theoretical estimates for the $D_0(M_{12} - M)$ and $D_0(M_{12}^+ - M)$ energies corresponding to the removal of a single atom from the M_{13} and M_{13}^+ clusters, respectively, are compared in Table V. Our theoretical values are computed as

$$D_0\left(M_{12}^{0,+} - M\right) = E_{tot}^{el}\left(M_{12}^{0,+}\right) + \mathrm{ZPVE}\left(M_{12}^{0,+}\right) + E_{tot}(M) - \left[E_{tot}^{el}\left(M_{13}^{0,+}\right) + \mathrm{ZPVE}\left(M_{13}^{0,+}\right)\right]. \quad (5)$$

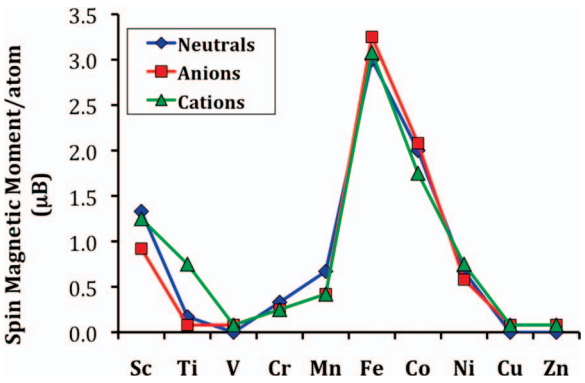

FIG. 8. Spin magnetic moment per atom (in μ_B) in the M_{12} series.

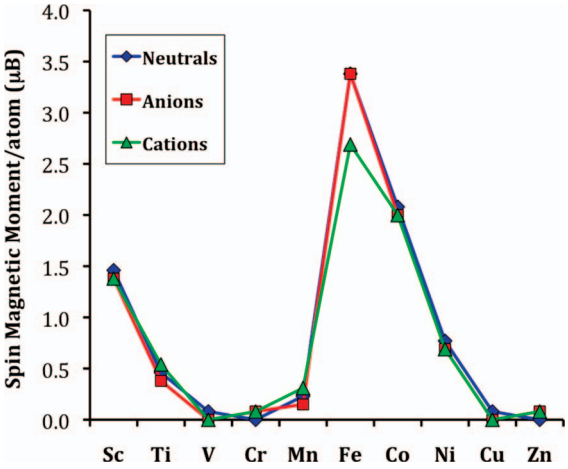

FIG. 9. Spin magnetic moment per atom (in μ_B) in the M_{13} series.

TABLE V. Single atom removal energies of M_{13} and M_{13}^+. All values are in eV.

	Sc_{13}	Ti_{13}	V_{13}	Cr_{13}	Mn_{13}	Fe_{13}	Co_{13}	Ni_{13}	Cu_{13}	Zn_{13}
$2S+1$	20	7	2	1	4	45	28	11	2	1
$M_{12}-M$	4.24	4.72	3.58	2.77	3.05	3.79	3.85	3.26	2.28	0.45
Exper.			4.63 ± 0.33[a]			4.32 ± 0.15[b] 4.11 ± 0.37[c]	3.68 ± 0.31[d]	3.45 ± 0.40[e]		
M_{12}^+-M	4.04	4.68	3.79	2.66	3.02	3.62	3.91	3.29	2.83	0.45
Exper.		4.66 ± 0.41[f]	4.65 ± 0.32[a] 4.35 ± 0.13[g]	3.00 ± 0.24[h]		4.02 ± 0.47[c]	3.64 ± 0.30[d]	3.44 ± 0.39[e]	3.42 ± 0.23[i]	

[a]See Ref. 136.
[b]See Ref. 160.
[c]See Ref. 139.
[d]See Ref. 142.
[e]See Ref. 161.
[f]See Ref. 157.
[g]See Ref. 158.
[h]See Ref. 159.
[i]See Ref. 162.

The theoretical values are in relatively good agreement with the experiment. The difference between theory and experiment is within 0.5 eV if the experimental uncertainty bars are taken into account.

In order to compare binding energies per atom with the corresponding bulk values, we computed atomization energies of the neutral M_{12} and M_{13} clusters according to the expression

$$E_{\text{atom}}(n) = \left[E_{\text{tot}}{}^{\text{el}}(M_n) + \text{ZPVE}(M_n) - nE_{\text{tot}}(M)\right]/n. \quad (6)$$

The values computed according to Eqs. (5) and (6) are presented in Fig. 10 together with the dissociation energies of the M_2 dimers, M = Sc−Zn computed[133,134] at the same BPW91/6-311+G* level, and bulk cohesive energies.[135] The dimer dissociation energies correspond to the smallest values for a given atom except for V, Cu, and Zn where the dimer dissociation energies are close to the atomization energies of V_n, Cu_n, and Zn_n, respectively. The $M_{12} - M$ dissociation energies are closer to the corresponding bulk cohesive energies than the atomization energies and match the bulk values at V and Cr. All the curves possess the maxima at Ti, V, Fe, Ni, and Co (see the supplementary material[163]).

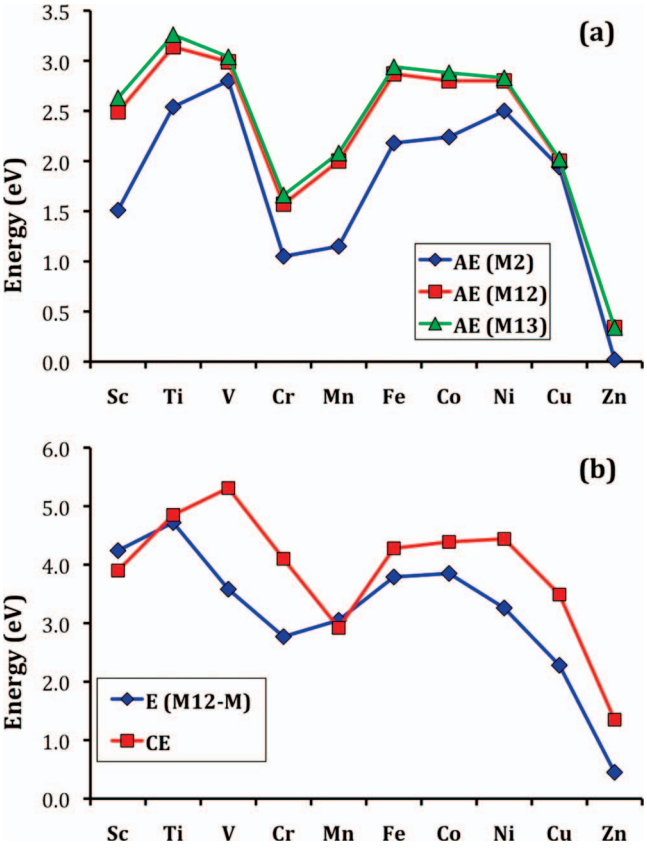

FIG. 10. Atomization energies for the lowest total energy states in the M_2, M_{12}, and M_{13} series, the atom removal energies in the M_{13} series, and cohesive energies in the M bulk: (a) AE(M_2) are the atomization energies of the M_2 dimers; AE(M_{12}) are the atomization energies of M_{12}; AE(M_{13}) are the atomization energies of M_{13}; (b) $E(M_{12} - M)$ are the $M_{12} - M$ dissociation energies; CE are the bulk cohesive energies.

IV. CONCLUSION

We performed a systematic study of the structure, stability, electronic and magnetic properties of the neutral and singly negatively and positively charged 12- and 13-atom clusters of all 3*d*-metals from Sc to Zn using all-electron density functional theory with generalized gradient approximation. The main results obtained can be summarized as follows:

(a) A number of members in the M_{12}, M_{12}^-, M_{12}^+, M_{13}, M_{13}^-, and M_{13}^+ series (M = Sc−Zn) possesses multiple states which are close in total energy to the lowest total energy state. Several such cases were analyzed using larger basis sets and/or other exchange-correlation functionals. The results obtained using a larger basis set were qualitatively the same as those obtained using the 6-311+G* basis set.

(b) The lowest total energy states of the ions possess geometrical configurations that are different from those of their corresponding neutral parents in the V_{13}, Mn_{12}, Co_{12}, Ni_{13}, Cu_{13}, Zn_{12}, and Zn_{13} series.

(c) The one-electron rule according to which an electron detachment or attachment from/to a neutral species results in the change of $\pm 1.0\ \mu_B$ in the total spin magnetic

moment is valid in all cases except for Sc_{12}^-, Ti_{12}^+, Mn_{12}^-, Mn_{12}^+, Fe_{12}^-, Fe_{13}^+, and Co_{12}^+.

(d) Our computed ionization energies of the neutrals and vertical detachment energies of the anions are within 0.1 eV from the experimental values if the experimental uncertainty bars are taken into account. Thus, the BPW91/6-311+G^* level of theory applied in the present work can be considered to be quite reliable.

(e) The computed energies of a single atom removal [$D_0(M_{12} - M)$ and $D_0(M_{12}^+ - M)$] are in satisfactory agreement with the experimental values possessing quite large uncertainty bars. The $D_0(M_{12} - M)$ dissociation energies are found to be significantly larger than the dissociation energies of the M_2 dimers and to be close to the corresponding bulk cohesive energies. In particular, the $D_0(Ti_{12} - Ti)$ and $D_0(Mn_{12} - Mn)$ values agree well with the corresponding bulk cohesive energies.

ACKNOWLEDGMENTS

This research was partially supported by a grant from the (U.S.) Department of Energy (DOE). G.L.G. and C.A.W. were partially supported by the National Science Foundation (NSF) cooperative agreement 0630370 (CREST Center for Astrophysical Science and Technology). B.R.R. acknowledges support by the National Science Foundation through Grant No. EPS-1003897. Portions of this research were conducted with high performance computational resources provided by the Louisiana Optical Network Initiative (http://www.loni.org).

[1] P. Jena and A. W. Castleman, Jr., Proc. Natl. Acad. Sci. U.S.A. **103**, 10560 (2006).
[2] M. Sakurai, K. Watanabe, K. Sumiyama, and K. Suzuki, J. Chem. Phys. **111**, 235 (1999).
[3] Y. Sun, M. Zhang, and R. Fournier, Phys. Rev. B **77**, 075435 (2008).
[4] F. Aguilera-Granja, L. C. Balbás, and A. Vega, J. Phys. Chem. A **113**, 13483 (2009).
[5] Y. Sun, R. Fournier, and M. Zhang, Phys. Rev. A **79**, 043202 (2009).
[6] M. Zhang and R. Fournier, Phys. Rev. A **79**, 043203 (2009).
[7] M. J. Piotrowski, P. Piquini, and J. L. F. Da Silva, Phys. Rev. B **81**, 155446 (2010).
[8] M. J. Piotrowski, P. Piquini, M. M. Odashima, and J. L. F. Da Silva, J. Chem. Phys. **134**, 134105 (2011).
[9] A. D. Becke, Phys. Rev. A **38**, 3098 (1988).
[10] J. P. Perdew and Y. Wang, Phys. Rev. B **45**, 13244 (1992).
[11] G. L. Gutsev, B. K. Rao, and P. Jena, J. Phys. Chem. A **104**, 11961 (2000).
[12] G. L. Gutsev, C. A. Weatherford, K. Pradhan, and P. Jena, J. Phys. Chem. A **114**, 9014 (2010).
[13] K. Pradhan, G. L. Gutsev, C. A. Weatherford, and P. Jena, J. Chem. Phys. **134**, 144305 (2011).
[14] G. L. Gutsev and C. W. Bauschlicher, Jr., J. Phys. Chem. A **107**, 7013 (2003).
[15] R. J. Bartlett and M. Musial, Rev. Mod. Phys. **79**, 291 (2007).
[16] S. Li and D. A. Dixon, J. Phys. Chem. A **112**, 6646 (2008).
[17] H.-J. Zhai, S. Li, D. A. Dixon, and L.-S. Wang, J. Am. Chem. Soc. **130**, 5167 (2008).
[18] S. Li, J. M. Hennigan, D. A. Dixon, and K. A. Peterson, J. Phys. Chem. A **113**, 7861 (2009).
[19] F. Grein, Int. J. Quantum Chem. **109**, 549 (2009).
[20] S. Li, H.-J. Zhai, L.-S. Wang, and D. A. Dixon, J. Phys. Chem. A **113**, 11273 (2009).
[21] C. J. Cramer and D. G. Truhlar, Phys. Chem. Chem. Phys. **11**, 10757 (2009).
[22] K. Yang, J. Zheng, Y. Zhao, and D. G. Truhlar, J. Chem. Phys. **132**, 164117 (2010).
[23] R. Krishnan, J. S. Binkley, R. Seeger, and J. A. Pople, J. Chem. Phys. **72**, 650 (1980).
[24] L. A. Curtiss, M. P. McGrath, J.-P. Blaudeau, N. E. Davis, R. C. Binning, Jr., and L. Radom, J. Chem. Phys. **103**, 6104 (1995).
[25] M. J. Frisch, G. W. Trucks, H. B. Schlegel *et al.*, GAUSSIAN 09, Revision A.1-C.1, Gaussian, Inc., Wallingford, CT, 2009.
[26] A. E. Reed, L. A. Curtiss, and F. Weinhold, Chem. Rev. **88**, 899 (1988).
[27] M. B. Knickelbein, Phys. Rev. B **71**, 184442 (2005).
[28] H. K. Yuan, H. Chen, A. S. Ahmed, and J. F. Zhang, Phys. Rev. B **74**, 144434 (2006).
[29] J. Wang, Phys. Rev. B **75**, 155422 (2007).
[30] G. Wu, J. Wang, Y. Lu, and M. Yang, J. Chem. Phys. **128**, 224315 (2008).
[31] J. Wang, Y. Wang, G. Wu, X. Zhang, X. Zhao, and M. Yang, Phys. Chem. Chem. Phys. **11**, 5980 (2009).
[32] F.-Y. Tian and Y.-X. Wang, Int. J Quantum Chem. **110**, 1573 (2010).
[33] Y. Wang, G. Wu, J. Du, M. Yang, and J. Wang, J. Phys. Chem. A **116**, 93 (2012).
[34] J. Zhao, Q. Qiu, B. Wang, J. Wang, and G. Wang, Solid State Commun. **118**, 157 (2001).
[35] M. Castro, S.-R. Liu, H.-J. Zhai, and L.-S. Wang, J. Chem. Phys. **118**, 2116 (2003).
[36] S.-Y. Wang, J.-Z. Yu, H. Mizuseki, J.-A. Yan, Y. Kawazoe, and C.-Y. Wang, J. Chem. Phys. **120**, 8463 (2004).
[37] T. J. D. Kumar, P. Tarakeshwar, and N. Balakrishnan, Phys. Rev. B **79**, 205415 (2009).
[38] M. Salazar-Villanueva, P. H. H. Tejeda, U. Pal, J. F. Rivas-Silva, J. I. R. Mora, and J. A. Ascencio, J. Phys. Chem. A **110**, 10274 (2006).
[39] J.-O. Joswig and M. Springborg, J. Phys.: Condens. Matter **19**, 106207 (2007).
[40] A. N. Chibisov, "First principles calculations of the agglomeration of Ti nanoparticles," Mater. Lett. (in press).
[41] T. J. D. Kumar, P. F. Weck, and N. Balakrishnan, J. Phys. Chem. C **111**, 7494 (2007).
[42] M. S. Villanueva, A. H. Romero, and A. B. Hernández, Nanotechnology **20**, 465709 (2009).
[43] A. N. Kravtsova, A. A. Guda, V. L. Mazalova, A. V. Soldatov, and R. L. Johnston, Nanostruct.: Math. Phys. Model. **4**, 15 (2011) (in Russian).
[44] J. Medina, R. de Coss, A. Tapia, and G. Canto, Eur. Phys. J. B **76**, 427 (2010).
[45] S.-Y. Wang, W. Duan, D.-L. Zhao, and C.-Y. Wang, Phys. Rev. B **65**, 165424 (2002).
[46] A. Taneda, T. Shimizu, and Y. Kawazoe, J. Phys.: Condens. Matter **13**, L305 (2001).
[47] G. Wu, M. Yang, X. Guo, and J. Wang, J. Comput. Chem. **33**, 1854 (2012).
[48] C. Ratsch, A. Fielicke, A. Kirilyuk, J. Behler, G. von Helden, G. Meijer, and M. Scheffler, J. Chem. Phys. **122**, 124302 (2005).
[49] H. Cheng and L.-S. Wang, Phys. Rev. Lett. **77**, 51 (1996).
[50] B. V. Reddy, S. N. Khanna, and P. Jena, Phys. Rev. B **60**, 15597 (1999).
[51] S. K. Nayak, M. Nooijen, and P. Jena, J. Phys. Chem. A **103**, 9853 (1999).
[52] T. M. Briere, M. H. F. Sluiter, V. Kumar, and Y. Kawazoe, Phys. Rev. B **66**, 064412 (2002).
[53] P. Bobadova-Parvanova, K. A. Jackson, S. Srinivas, and M. Horoi, Phys. Rev. A **67**, 061202(R) (2003).
[54] O. Gourdon and G. J. Miller, J. Solid State Chem. **173**, 137 (2003).
[55] S. Datta, M. Kabir, A. Mookerjee, and T. Saha-Dasgupta, Phys. Rev. B **83**, 075425 (2011).
[56] G. L. Gutsev, M. D. Mochena, C. W. Bauschlicher, Jr., W.-J. Zheng, O. C. Thomas, and K. H. Bowen, J. Chem. Phys. **129**, 044310 (2008).
[57] R. C. Longo, J. Carrete, and L. J. Gallego, J. Chem. Phys. **131**, 046101 (2009).
[58] P. Bobadova-Parvanova, K. A. Jackson, S. Srinivas, and M. Horoi, J. Chem. Phys. **122**, 014310 (2005).
[59] M. Kabir, A. Mookerjee, and D. G. Kanhere, Phys. Rev. B **73**, 224439 (2006).
[60] A. N. Andriotis and M. Menon, Phys. Rev. B **57**, 10069 (1998).
[61] O. Diéguez, M. M. G. Alemany, C. R. P. Ordejón, and L. J. Gallego, Phys. Rev. B **63**, 205407 (2001).
[62] P. Bobadova-Parvanova, K. A. Jackson, S. Srinivas, and M. Horoi, Phys. Rev. B **66**, 195402 (2002).
[63] C. Köhler, G. Seifert, and T. Frauenheim, Chem. Phys. **309**, 23 (2005).
[64] G. Rollmann, P. Entel, and S. Sahoo, Comput. Mater. Sci. **35**, 275 (2006).
[65] G. Rollmann, M. E. Gruner, A. Hucht, R. Meyer, P. Entel, M. L. Tiago, and J. R. Chelikowsky, Phys. Rev. Lett. **99**, 083402 (2007).

[66]Q.-M. Ma, Z. Xie, J. Wang, Y. Liu, and Y.-C. Li, Solid State Commun. **142**, 114 (2007).
[67]O. Šipr, M. Košuth, and H. Ebert, Phys. Rev. B **70**, 174423 (2004).
[68]S. Sahoo, A. Hucht, M. E. Gruner, G. Rollmann, P. Entel, A. Postnikov, J. Ferrer, L. Fernández-Seivane, M. Richter, D. Fritsch, and S. Sil, Phys. Rev. B **82**, 054418 (2010).
[69]G. L. Gutsev, C. A. Weatherford, P. Jena, E. Johnson, and B. R. Ramachandran, J. Phys. Chem. C **116**, 7050 (2012).
[70]G. L. Gutsev, C. A. Weatherford, P. Jena, E. Johnson, and B. R. Ramachandran, J. Phys. Chem. A **116**, 10218 (2012).
[71]M. Niemeyer, K. Hirsch, V. Zamudio-Bayer, A. Langenberg, M. Vogel, M. Kossick, C. Ebrecht, K. Egashira, A. Terasaki, T. Möller, B. v. Issendorff, and J. T. Lau, Phys. Rev. Lett. **108**, 057201 (2012).
[72]M. Wu, A. K. Kandalam, G. L. Gutsev, and P. Jena, Phys. Rev. B **86**, 174410 (2012).
[73]Z.-Q. Li and B.-L. Gu, Phys. Rev. B **47**, 13611 (1993).
[74]K. Miura, H. Kimura, and S. Imanaga, Phys. Rev. B **50**, 10335 (1994).
[75]H. M. Duan and Q. Q. Zheng, Phys. Lett. A **280**, 333 (2001).
[76]J. L. Rodríguez-López, F. Aguilera-Granja, K. Michaelian, and A. Vega, Phys. Rev. B **67**, 174413 (2003).
[77]Q.-M. Ma, Z. Xie, J. Wang, Y. Liu, and Y.-C. Li, Phys. Lett. A **358**, 289 (2006).
[78]Q. M. Ma, Y. Liu, Z. Xie, and J. Wang, J. Phys.: Conf. Ser. **29**, 163 (2006).
[79]S. Rives, A. Catherinot, F. Dumas-Bouchiat, C. Champeaux, A. Videcoq, and R. Ferrando, Phys. Rev. B **77**, 085407 (2008).
[80]C. D. Dong and X. G. Gong, Phys. Rev. B **78**, 020409(R) (2008).
[81]F. Aguilera-Granja, A. García-Fuente, and A. Vega, Phys. Rev. B **78**, 134425 (2008).
[82]M. J. Piotrowski, P. Piquini, L. Cândido, and J. L. F. Da Silva, Phys. Chem. Chem. Phys. **13**, 17242 (2011).
[83]P. L. Tereshchuk, Comput. Mater. Sci. **50**, 991 (2011).
[84]J. Lv, F.-Q. Zhang, J.-F. Jia, X.-H. Xu, and H.-S. Wu, J. Mol. Struct: THEOCHEM **955**, 14 (2010).
[85]S. Datta, M. Kabir, S. Ganguly, B. Sanyal, T. Saha-Dasgupta, and A. Mookerjee, Phys. Rev. B **76**, 014429 (2007).
[86]G. M. Pastor, J. Dorantes-Dávila, and K. H. Bennemann, Phys. Rev. B **40**, 7642 (1989).
[87]F. A. Reuse and S. N. Khanna, Chem. Phys. Lett. **234**, 77 (1995).
[88]F. A. Reuse, S. N. Khanna, and S. Bernel, Phys. Rev. B **52**, R11650 (1995).
[89]S. K. Nayak, S. N. Khanna, B. K. Rao, and P. Jena, J. Phys. Chem. A **101**, 1072 (1997).
[90]B. V. Reddy, S. K. Nayak, S. N. Khanna, B. K. Rao, and P. Jena, J. Phys. Chem. A **102**, 1748 (1998).
[91]M. Calleja, C. Rey, M. M. G. Alemany, L. J. Gallego, P. Ordejón, D. Sánchez-Portal, E. Artacho, and J. M. Soler, Phys. Rev. B **60**, 2020 (1999).
[92]J. A. Alonso, Chem. Rev. **100**, 637 (2000).
[93]V. G. Grigoryan and M. Springborg, Phys. Rev. B **70**, 205415 (2004).
[94]T. Futschek, J. Hafner, and M. Marsman, J. Phys.: Condens. Matter **18**, 9703 (2006).
[95]B. Lee and G. W. Lee, J. Chem. Phys. **127**, 164316 (2007).
[96]Y. H. Yao, X. Gu, M. Ji, X. G. Gong, and D.-S. Wang, Phys. Lett. A **360**, 629 (2007).
[97]J. P. Chou, H. Y. T. Chen, C. R. Hsing, C. M. Chang, C. Cheng, and C. M. Wei, Phys. Rev. B **80**, 165412 (2009).
[98]P. Błónski and J. Hafner, J. Phys.: Condens. Matter **23**, 136001 (2011).
[99]W. Song, W.-C. Lu, C. Z. Wang, and K. M. Ho, Comput. Theor. Chem. **978**, 41 (2011).
[100]C. Zhou, S. Yao, Q. Zhang, J. Wu, M. Yang, R. C. Forrey, and H. Cheng, J. Mol. Model. **17**, 2305 (2011).
[101]R. Singh and P. Kroll, Phys. Rev. B **78**, 245404 (2008).
[102]Q. L. Lu, Q. Q. Luo, L. L. Chen, and J. G. Wan, Eur. Phys. J. D **61**, 389–396 (2011).
[103]J. P. Perdew, K. Burke, and M. Ernzerhof, Phys. Rev. Lett. **77**, 3865 (1996).
[104]J. M. Tao, J. P. Perdew, V. N. Staroverov, and G. E. Scuseria, Phys. Rev. Lett. **91**, 146401 (2003).
[105]Y. Zhao and D. G. Truhlar, J. Chem. Phys. **125**, 194101 (2006).
[106]P. B. Balbuena, P. A. Derosa, and J. M. Seminario, J. Phys. Chem. B **103**, 2830 (1999).
[107]J. Oviedo and R. E. Palmer, J. Chem. Phys. **117**, 9548 (2002).
[108]E. M. Fernández, J. M. Soler, I. L. Garzón, and L. C. Balbás, Phys. Rev. B **70**, 165403 (2004).
[109]D. Alamanova, V. G. Grigoryan, and M. Springborg, J. Phys.: Condens. Matter **19**, 346204 (2007).
[110]M. Kabir, A. Mookerjee, and A. K. Bhattacharya, Phys. Rev. A **69**, 043203 (2004).
[111]Q. L. Lu, L. Z. Zhu, L. Ma, and G. H. Wang, Chem. Phys. Lett. **407**, 176 (2005).
[112]J. Mejía-López, G. García, and A. H. Romero, J. Chem. Phys. **131**, 044701 (2009).
[113]G. Guzmán-Ramírez, F. Aguilera-Granja, and J. Robles, Eur. Phys. J. D **57**, 49 (2010).
[114]K. Baishya, J. C. Idrobo, S. Ögüt, M. Yang, K. A. Jackson, and J. Jellinek, Phys. Rev. B **83**, 245402 (2011).
[115]X. Chu, M. Xiang, Q. Zeng, W. Zhu, and M. Yang, J. Phys. B **44**, 205103 (2011).
[116]M. Yang, F. Yang, K. A. Jackson, and J. Jellinek, J. Chem. Phys. **132**, 064306 (2010).
[117]Q. Zeng, X. Wang, M. L. Yang, and H. B. Fu, Eur. Phys. J. D **58**, 125 (2010).
[118]J. Wang, G. Wang, and J. Zhao, Phys. Rev. A **68**, 013201 (2003).
[119]K. Iokibe, H. Tachikawa, and K. Azumi, J. Phys. B **40**, 427 (2007).
[120]F. W. Payne, W. Jiang, and L. A. Bloomfield, Phys. Rev. Lett. **97**, 193401 (2006).
[121]M. B. Knickelbein, Phys. Rev. Lett. **86**, 5255 (2001).
[122]M. B. Knickelbein, Chem. Phys. Lett. **353**, 221 (2002).
[123]I. M. L. Billas, J. A. Becker, A. Chatelain, and W. A. de Heer, Phys. Rev. Lett. **71**, 4067 (1993).
[124]J. P. Bucher, D. C. Douglass, and L. A. Bloomfield, Phys. Rev. Lett. **66**, 3052 (1991).
[125]X. Xu, S. Yin, R. Moro, and W. A. de Heer, Phys. Rev. Lett. **95**, 237209 (2005).
[126]M. B. Knickelbein, J. Chem. Phys. **125**, 044308 (2006).
[127]F. W. Payne, W. Jiang, J. W. Emmert, J. Deng, and L. A. Bloomfield, Phys. Rev. B **75**, 094431 (2007).
[128]I. M. L. Billas, A. Châtelain, and W. A. de Heer, Science **265**, 1682 (1994).
[129]S. E. Apsel, J. W. Emmert, J. Deng, and L. A. Bloomfield, Phys. Rev. Lett. **76**, 1441 (1996).
[130]S. Peredkov, M. Neeb, W. Eberhardt, J. Meyer, M. Tombers, H. Kampschulte, and G. Niedner-Schatteburg, Phys. Rev. Lett. **107**, 233401 (2011).
[131]X. Xu, S. Yin, R. Moro, A. Liang, J. Bowlan, and W. A. de Heer, Phys. Rev. Lett. **107**, 057203 (2011).
[132]R. A. Guirado-López, J. Dorantes-Dávila, and G. M. Pastor, "Orbital magnetism in transition-metal clusters: From Hund's rules to bulk quenching," Phys. Rev. Lett. **90**, 226402 (2003).
[133]G. L. Gutsev and C. W. Bauschlicher, Jr., J. Phys. Chem. A **107**, 4755 (2003).
[134]G. L. Gutsev, M. D. Mochena, P. Jena, C. W. Bauschlicher, Jr., and H. Partridge III, J. Chem. Phys. **121**, 6785 (2004).
[135]P. H. T. Philipsen and E. J. Baerends, Phys. Rev. B **54**, 5326–5333 (1996).
[136]C. X. Su, D. A. Hales, and P. B. Armentrout, J. Chem. Phys. **99**, 6613 (1993).
[137]M. B. Knickelbein, Phys. Rev. A **67**, 013202 (2003).
[138]G. M. Koretsky and M. B. Knickelbein, J. Chem. Phys. **106**, 9810 (1997).
[139]L. Lian, C.-X. Su, and P. B. Armentrout, J. Chem. Phys. **97**, 4072 (1992).
[140]S. Yang and M. B. Knickelbein, J. Chem. Phys. **93**, 1533 (1990).
[141]E. K. Parks, T. D. Klots, and S. J. Riley, J. Chem. Phys. **92**, 3813 (1990).
[142]D. A. Hales, C.-X. Su, L. Lian, and P. B. Armentrout, J. Chem. Phys. **100**, 1049 (1994).
[143]M. B. Knickelbein, S. Yang, and S. J. Riley, J. Chem. Phys. **93**, 94 (1990).
[144]M. B. Knickelbein, Chem. Phys. Lett. **192**, 129 (1992).
[145]S.-R. Liu, H.-J. Zhai, M. Castro, and L.-S. Wang, J. Chem. Phys. **118**, 2108 (2003).
[146]H. Wu, S. R. Desai, and L.-S. Wang, Phys. Rev. Lett. **77**, 2436 (1996).
[147]M. Iseda, T. Nishio, S. Y. Han, H. Yoshida, A. Terasaki, and T. Kondow, J. Chem. Phys. **106**, 2182 (1997).
[148]L.-S. Wang, H. Wu, and H. Cheng, Phys. Rev. B **55**, 12884 (1997).
[149]L.-S. Wang, H. S. Cheng, and J. Fan, J. Chem. Phys. **102**, 9480 (1995).
[150]L.-S. Wang, X. Li, and H. F. Zhang, Chem. Phys. **262**, 53 (2000).
[151]S.-R. Liu, H.-J. Zhai, and L.-S. Wang, Phys. Rev. B **64**, 153402 (2001).
[152]S.-R. Liu, H.-J. Zhai, and L.-S. Wang, J. Chem. Phys. **117**, 9758 (2002).
[153]C. L. Pettiette, S. H. Yang, M. J. Craycraft, J. Conceicao, R. T. Laaksonen, O. Cheshnovsky, and R. E. Smalley, J. Chem. Phys. **88**, 5377 (1988).
[154]K. J. Taylor, C. L. Pettiette-Hall, O. Cheshnovsky, and R. E. Smalley, J. Chem. Phys. **96**, 3319 (1992).
[155]C.-Y. Cha, G. Ganteför, and W. Eberhardt, J. Chem. Phys. **99**, 6308 (1993).

[156]O. Kostko, G. Wrigge, O. Cheshnovsky, and B. v. Issendorff, J. Chem. Phys. **123**, 221102 (2005).
[157]L. Lian, C. X. Su, and P. B. Armentrout, J. Chem. Phys. **97**, 4084 (1992).
[158]K. Hansen, A. Herlert, L. Schweikhard, M. Vogel, and C. Walther, Eur. Phys. J. D **34**, 67 (2005).
[159]C. X. Su and P. B. Armentrout, J. Chem. Phys. **99**, 6506 (1993).
[160]P. B. Armentrout, Annu. Rev. Phys. Chem. **52**, 423 (2001).
[161]L. Lian, C. X. Su, and P. B. Armentrout, J. Chem. Phys. **96**, 7542 (1992).
[162]S. Krückeberg, L. Schweikhard, J. Ziegler, G. Dietrich, K. Lützenkirchen, and C. Walther, J. Chem. Phys. **114**, 2955 (2001).
[163]See supplementary material at http://dx.doi.org/10.1063/1.4799917 for two files (M_{12} and M_{13}) containing the short outputs of all 60 lowest total energy states shown in the figures. Each output provides optimized coordinates, harmonic frequencies, NAO populations, and total energies.